SIMULATION OF TURBULENT FLOW AND HEAT TRANSFER OVER A BACKWARD-FACING STEP WITH RIBS TURBULATORS

by

Khudheyer S. MUSHATET

Mechanical Engineering Department, College of Engineering, Thi-qar University, Nassiriya, Iraq

Original scientific paper
UDC: 532.517.4:536.24
DOI: 10.2298/TSCI090926044M

Simulation is presented for a backward-facing step flow and heat transfer inside a channel with ribs turbulators. The problem was investigated for Reynolds numbers up to 32000. The effect of a step height, the number of ribs and the rib thickness on the flow and thermal field were investigated. The computed results are presented as streamlines counters, velocity vectors, and graphs of Nusselt number and turbulent kinetic energy variation. A control volume method employing a staggered grid techniques was imposed to discretize the governing continuity, full Navier-Stockes and energy equations. A computer program using a SIMPLE algorithm was developed to handle the considered problem. The effect of turbulence was modeled by using a k-ε model with its wall function formulas. The obtained results show that the strength and size of the recirculation zones behind the step are increased with the increase of contraction ratio (i. e. with the increase of a step height). The size of recirculation regions and the reattachment length after the ribs are decreased with increasing of the contraction ratio. Also the results show that the Reynolds number and contraction ratio have a significant effect on the variation of turbulent kinetic energy and Nusselt number.

Keywords: *backward facing, ribs, turbulent duct flow*

Introduction

A backward-facing step channel flow is considered an interesting topic for many researchers since it includes the phenomena of separation and reattachment. Ribs turbulators are widely used in some engineering applications such as serpentine cooling air channel for the internal cooling of the gas turbine, heat exchanges and cooling of electronic devices. In some applications, the control on the size and strength of the separation zone is needed to get the desired heat transfer. However the geometry is simple but it is still one of the problems that have a complex flow field. Thus extra work involving study of some changes on the considered geometry is needed to get a better understanding. In relating channels with a backward facing, many investigations has been reviewed. Lio *et al.* [1] performed a numerical investigation over a backward-facing. The emphasis in this study is given to the effect of abrupt expansion entrance on the local heat transfer characteristics. The obtained results show that the separation just after the step has a significant effect on heat transfer especially in the

* Authors; e-mail: khudheyer2004@yahoo.com

entrance region. Wang *et al*. [2] used a large eddy method along with Lagrangian approach to analyze the turbulent flow over a backward-facing step. The study showed that the particles follow a specified path when the vorticity of a gas phase is small. The effect of a step height on the separated flow for a convective flow adjacent to a backward-facing step was investigated numerically by Nie *et al*. [3], Thangam *et al*. [4]. Chen *et al.* [5] simulated the three dimensional laminar forced convection flow adjacent to inclined backward-facing step in a rectangular duct. The effect of a step inclination angle on the flow and heat transfer distribution was studied. An experimental study to visualize the turbulent separated flow and to measure the wall pressure over a backward-facing step was performed by Feng *et al*. [6]. The study show that the separation bubble and reattachment zone and the negative peak of the time-varying wall pressure was in phase with passage of the local large scale vertical structure. Concerning the channel flow with ribs, Han [7], Rau *et al.* [8], Web *et al*. [9], Lio *et al.* [10], and Hane *et al.* [11] investigated the turbulent flow in channels roughened with ribs. The aim of investigations was to predict the thermal field and friction factor. Five low turbulence models was used by Tsai *et al.* [12] to simulate the fully developed turbulent flow in a symmetric-ribbed channel. The results was validated with the work of Lio *et al.* [10]. Lacovides *et al.* [13] studied the flow and heat transfer in a rotating U-bend with inclined ribs. The study was performed for Reynolds number up to 36000 while the ribs angle of inclination was fixed by 45°.

In this paper, an attempt is made to incorporate the ribs turbulators (aliened in normal direction to the bottom wall of the channel) to the backward-facing flow. As shown in fig. 1, the bottom wall of the channel is hot (T_h = 50 °C) while the inlet channel flow was cold (T_c = 25 °C). The combined problem was investigated for different parameters such as the expansion ratio, the number of ribs, the rib thickness, and Reynolds number. To the knowledge of the researcher, there is no study documented on this flow situation up to date. So the objective of the present work is to show how the ribs turbulators can affect the conventional features of the turbulent flow and heat transfer of the backward-facing step in confined flows.

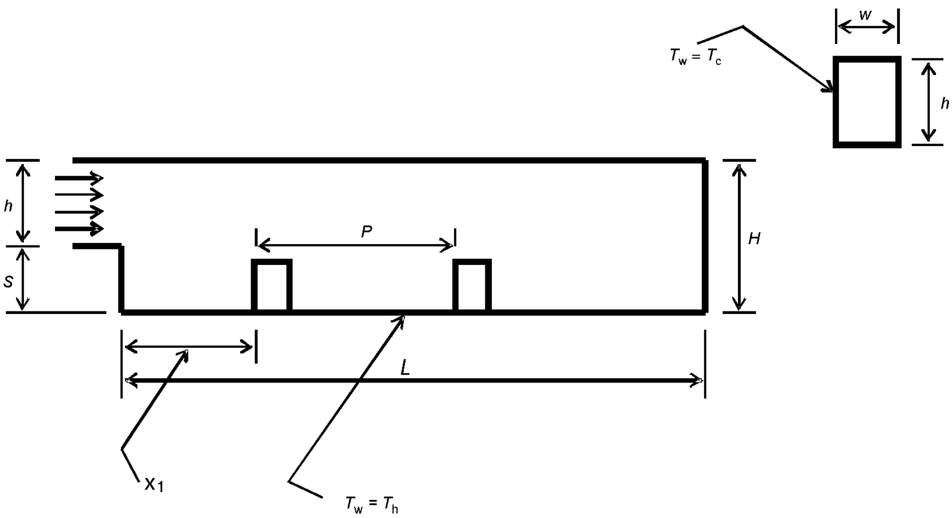

Figure 1. Schematic diagram of the considered problem, *H* = 0.05 m, *L* = 0.4 m, x_1 = 0.0492 m, *H/w* = 11, *P* = 0.1

Model description

The turbulent flow and heat transfer through a channel backward-facing step with rib turbulators are described by full Navier-Stockes, energy and continuity equations. The working fluid is an air with constant properties. The Boussinesq approximation is used. Thus, the mentioned governing equations are listed as:

$$\frac{\partial u}{\partial x}+\frac{\partial v}{\partial y}=0 \tag{1}$$

$$\rho u\frac{\partial u}{\partial x}+\rho v\frac{\partial u}{\partial y}=-\frac{\partial p}{\partial x}+2\frac{\partial}{\partial x}\left(\mu_{\text{eff}}\frac{\partial u}{\partial x}\right)+\frac{\partial}{\partial y}\left(\mu_{\text{eff}}\frac{\partial u}{\partial y}\right)+\frac{\partial}{\partial y}\left(\mu_{\text{eff}}\frac{\partial v}{\partial x}\right) \tag{2}$$

$$\rho u\frac{\partial v}{\partial x}+\rho v\frac{\partial v}{\partial y}=-\frac{\partial p}{\partial y}+\frac{\partial}{\partial x}\left(\mu_{\text{eff}}\frac{\partial v}{\partial x}\right)+2\frac{\partial}{\partial y}\left(\mu_{\text{eff}}\frac{\partial v}{\partial y}\right)+\frac{\partial}{\partial x}\left(\mu_{\text{eff}}\frac{\partial u}{\partial y}\right) \tag{3}$$

$$\rho u\frac{\partial T}{\partial x}+\rho v\frac{\partial T}{\partial y}=\frac{\partial}{\partial x}\left(\Gamma_{\text{eff}}\frac{\partial T}{\partial x}\right)+\frac{\partial}{\partial y}\left(\Gamma_{\text{eff}}\frac{\partial T}{\partial y}\right) \tag{4}$$

$$\mu_{\text{eff}}=\mu+\mu_{\text{t}} \tag{5}$$

$$\Gamma_{\text{eff, T}}=\frac{\mu}{\text{Pr}}+\frac{\mu_{\text{t}}}{\text{Pr}} \tag{6}$$

where μ_{eff} is the combined laminar and turbulent viscosity and Γ_{eff} is an effective exchange coefficient.

Turbulence model

The standard turbulence *k-ε* model proposed by Launder *et al*. [14] is adopted here to handle the effect of turbulence in the flow. This model includes two transport equations, one for turbulent kinetic energy and the other for the rate of dissipation of turbulent kinetic energy:

$$\rho u\frac{\partial k}{\partial x}+\rho v\frac{\partial k}{\partial y}=\frac{\partial}{\partial x}\left(\Gamma_{\text{eff},\,k}\frac{\partial k}{\partial x}\right)+\frac{\partial}{\partial y}\left(\Gamma_{\text{eff},\,\varepsilon}\frac{\partial k}{\partial y}\right)+\rho G-\rho\varepsilon \tag{7}$$

$$\rho u\frac{\partial \varepsilon}{\partial x}+\rho v\frac{\partial \varepsilon}{\partial y}=\frac{\partial}{\partial x}\left(\Gamma_{\text{eff},\,\varepsilon}\frac{\partial \varepsilon}{\partial x}\right)+\frac{\partial}{\partial y}\left(\Gamma_{\text{eff},\,\varepsilon}\frac{\partial \varepsilon}{\partial y}\right)+\rho C_{1\varepsilon}\frac{\varepsilon}{k}G+\rho C_{2\varepsilon}\frac{\varepsilon^2}{k} \tag{8}$$

where

$$G=\mu_{\text{t}}\left[2\left(\frac{\partial u}{\partial x}\right)^2+2\left(\frac{\partial v}{\partial y}\right)^2+\left(\frac{\partial u}{\partial y}+\frac{\partial v}{\partial x}\right)^2\right] \tag{9}$$

$$\Gamma_{\text{eff},\,k}=\frac{\mu_{\text{e}}}{\sigma_k},\quad \Gamma_{\text{eff},\,\varepsilon}=\frac{\mu_{\text{e}}}{\sigma_\varepsilon} \tag{10}$$

the eddy viscosity is obtained by the formula:

$$\mu_{\text{t}}=\rho C_\mu\frac{k^2}{\varepsilon} \tag{11}$$

and the model coefficients are: σ_k, σ_ε, $C_{1\varepsilon}$, $C_{2\varepsilon}$, and C_μ is 1.0, 1.3, 1.44, 1.92, and 0.09, respectively. The flow parameters at inlet are described as:

$$k_{\text{in}} = 0.05U_{\text{in}}^2, \quad T_{\text{in}} = T_{\text{c}} = 25\ °\text{C}$$
$$\varepsilon_{\text{in}} = \frac{k_{\text{in}}^{1.5}}{\lambda h}, \quad \lambda = 0.005 \tag{12}$$
$$\text{Re}_{\text{in}} = \frac{U_{\text{in}} h}{\upsilon}$$

where k_{in}, U_{in}, and T_{in}, are the turbulent kinetic energy, velocity, and temperature at a channel inlet, respectively.

At the walls, no slip conditions are imposed; $u = v = 0$, $k = 0$, $\partial\varepsilon/\partial y = 0$, $T_{\text{w}} = T_{\text{h}} = 50$ °C.

To treat the large steep gradient near the walls of the channel and step, wall function laws used by Versteege [15] is adopted. The local Nu along the bottom wall is expressed as Nu = $\partial\theta/\partial y$, at $y = 0$. Zero gradients are imposed on the channel exit for considered variables.

Numerical method

In this work, the numerical computations are performed on non-uniform staggered grid system. A finite volume method described by Versteege [15] is considered to integrate the equations from (1) to (5):

$$\int_{cv} (\rho\phi u)\text{d}v = \int_{cv} \text{div}(\Gamma \text{grad}\phi)\text{d}v + \int_{cv} S_\phi \text{d}v \tag{13}$$

This gives a system of discretization equations which means that the system of fully elliptic partial differential equations is transformed in a system of algebraic equations. Then the solution of these transformed equations is done by semi implicit line by line Guass elimination scheme. An elliptic finite volume computer code is developed to obtain the results of the numerical procedure through using pressure-velocity coupling (SIMPLE algorithm) [15]. This code is based on hybrid scheme. Because of this strong coupling and non-linearity inherent in these equations, relaxation factors are needed to ensure convergence. The relaxation factors used for velocity components, pressure, temperature, and turbulence quantities are 0.5, 0.8, 0.7, and 0.7, respectively. However these relaxation factors have been adjusted for each case studied to accelerate the convergence criterion defined as the relative deference of every dependent variable between iteration steps, $\max\left|\phi^{\text{k}}(i,j) - \phi^{\text{k}-1}(i,j)\right| \leq 10^{-5}$.

To ensure that the turbulent fluid flow solutions are not significantly effected by the mesh, the numerical simulations are examined under different grid sizes ranging from 62 × 28 until 82 × 52 control volumes. Any additional increase in grid points on 62 × 28 does not significantly effect on the results.

Results and discussion

Simulation of the backward-facing step flow with rib turbulators has been performed. The problem is investigated for different values of a step height (contraction ratio – *SR*) besides to the number of ribs for Reynolds number up to 32000. So the present results are summarized as follows.

Figures 2 and 3 show the flow field distribution for different values of contraction ratios and multiple rib turbulators. It can be seen that the boundary layer is separated just after the step forming a recirculating zone. The extension of this zone and reattachment are inhibited by the presence of the rib. So it can be emphasized that this zone is distorted due to the presence of the rib. The size and strength of this recirculation zone is increased with the increase of the step height as shown in (a) for the both mentioned figures and *vice versa* as shown in (b) and (c). After that, the flow is accelerated over the first rib along with the incoming main flow forming another recirculating zone. Also the reattachment is inhibited by the second rib and so on for the third rib. As a result the reattachment length is effected. It is clear that the size of the recirculation zone behind the first rib is larger compared with the other ribs. This will enhance the rate of heat transfer.

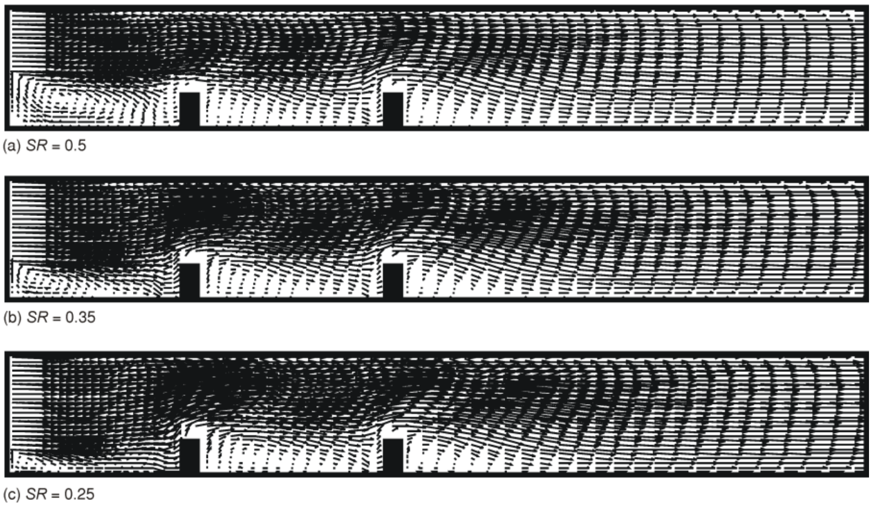

Figure 2. Computed velocity vectors for 2 ribs and different values of contraction ratios, Re = 16000, *H/w* = 11

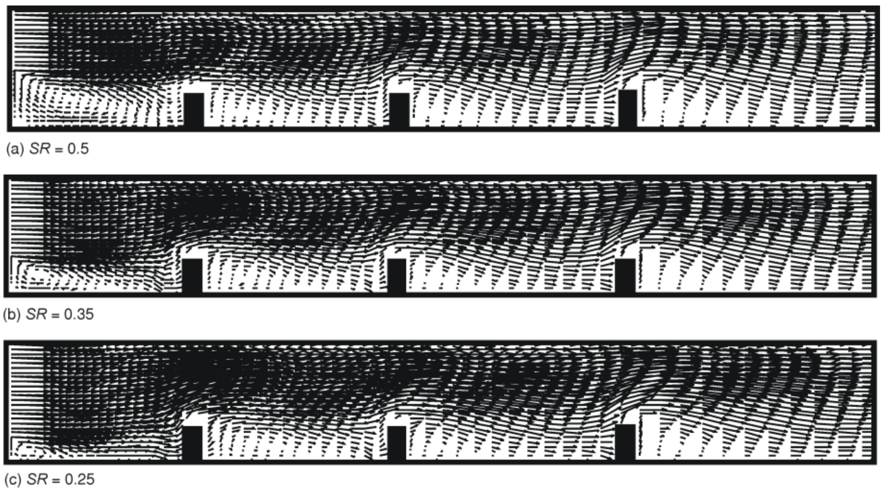

Figure 3. Computed velocity vectors for 3 ribs and different values of contraction ratios, Re = 16000, *H/w* = 11

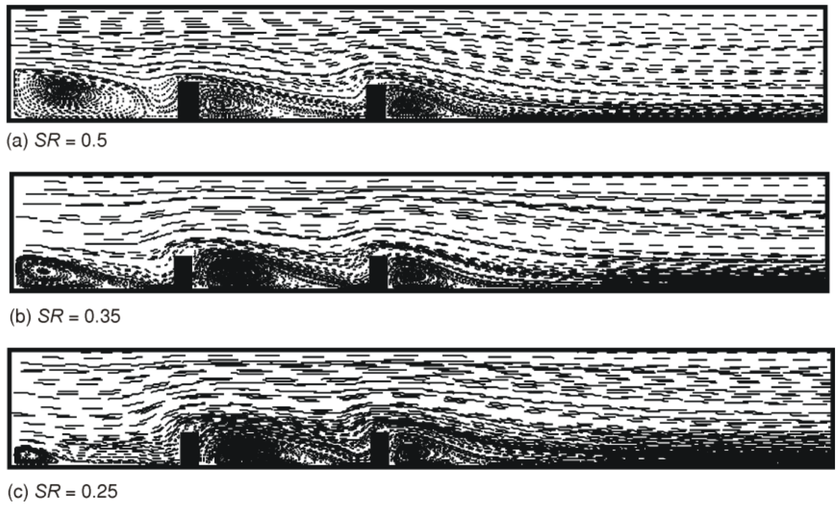

Figure 4. Stream lines distribution for 2 ribs and different values of contraction ratios, Re = 16000, *H/w* = 11

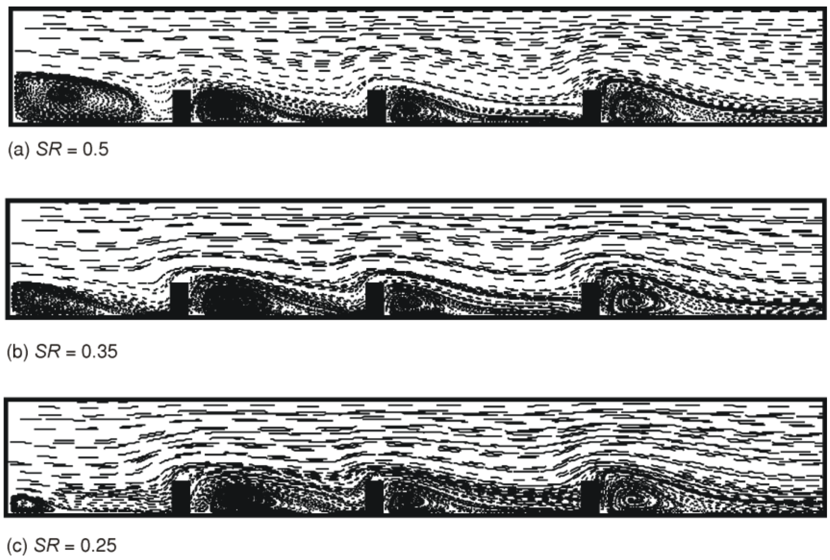

Figure 5. Stream lines distribution for 3 ribs and different values of contraction ratios, Re = 16000, *H/w* = 11

The stream lines distribution for the studied parameters is depicted in figs. 4 and 5. As can be mentioned in previous figures, the flow separates down stream the step and ribs forming a recirculation zone. The zone behind each rib works as a sudden expansion. The boundary layer attaches the wall of the channel at some distance down stream of the ribs. The presence of ribs will accelerate the flow and the recirculation zone seems to be larger at the first rib. The presence of ribs will promote mixing and enhance the rate of heat transfer as shown in fig. 9.

The distribution of axial velocity for different values of Re is depicted in fig. 6. As the Figure shows, the maximum values of the axial velocities are significantly increase with the increase of Re. This indicate that the strength of recirculation regions are increased with the increase of Re. The increase in Re, will increase the inertia force in the vicinity of the ribs creating a large re-circulating region downstream of the ribs. Consequently the rate of heat transfer will be enhanced as shown in fig. 10.

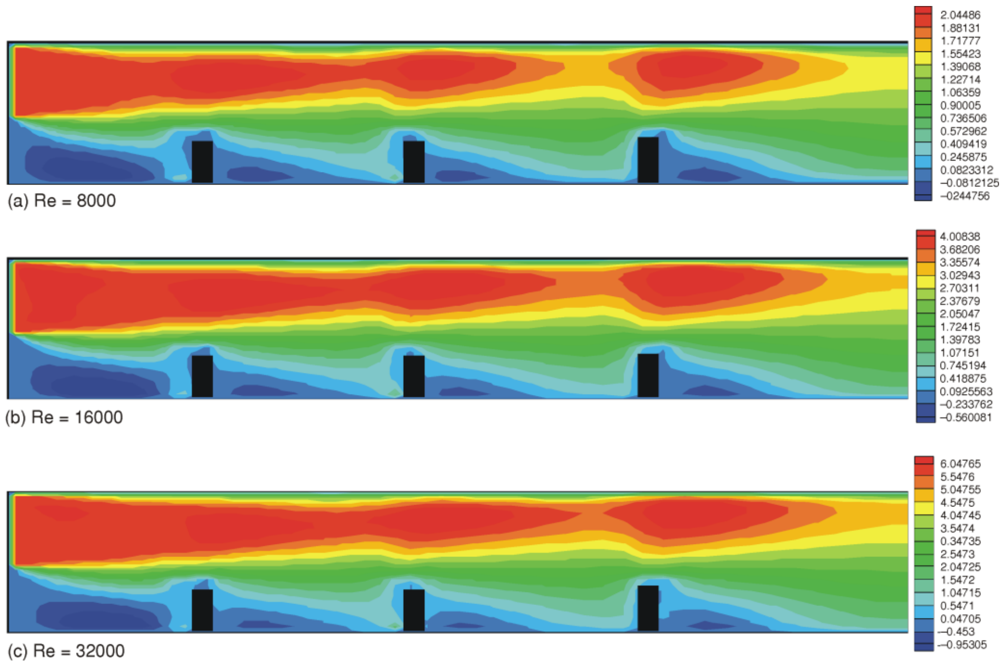

Figure 6. Effect of Re on distribution of axial velocity for 3 ribs, *SR* = 0.5, *H/w* = 11 (color image see on our web site)

Figure 7 shows the effect of Re on the variation of turbulent kinetic energy for three ribs and *SR* = 0.5. For the bottom wall at (a), the turbulent kinetic energy is significantly increased with the increase of Re and this increase is along the length of the channel. The maximum and minimum values of the turbulent kinetic energy (semi wavy variation) are due to the presence of rib turbulators. This distribution is changed when Re $\leq$ 8000. At the upper wall, (b), in which there is no ribs, the distribution of turbulent kinetic energy is some different where the maximum velocities over the ribs and the minimum velocities after the ribs affects the mentioned distribution. However the turbulent kinetic energy is increased with the increase of Re. At the middle of the channel, the turbulent kinetic energy is also increased with the increase of Re. However at Re = 8000, the distribution is similar to the bottom wall. The maximum values are larger than that of the bottom and upper wall because at the center of the channel, the maximum values of axial velocities are found and the stress is high, consequently the kinetic energy is increased. The effect of *SR* on the distribution of turbulent kinetic energy at the lower and upper wall of the channel is demonstrated at fig. 8. As the figure shows, the values of the turbulent kinetic energy are increased with the decrease of contraction. This may be due to

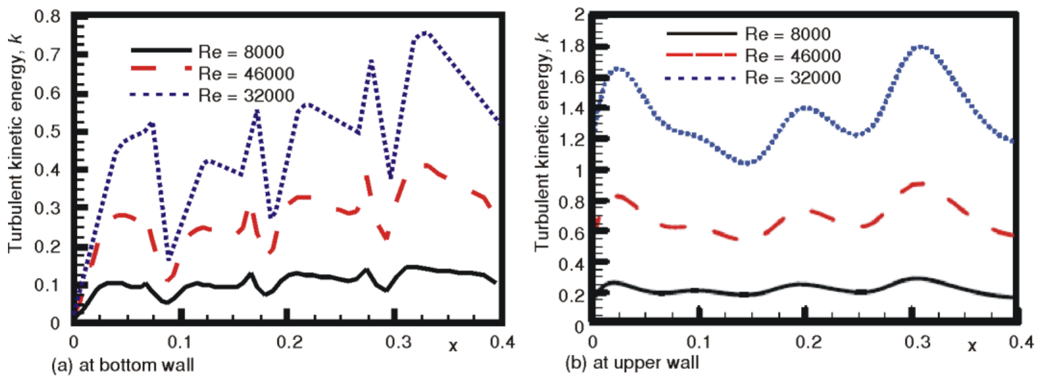

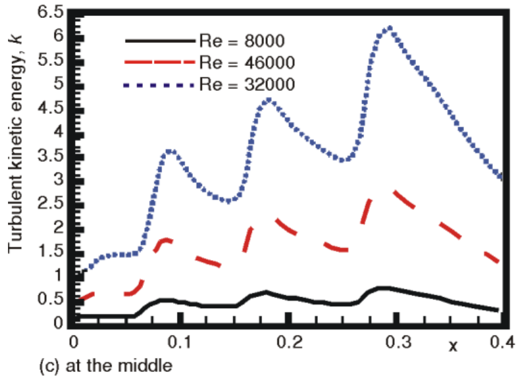

Figure 7. Effect of Re on variation of turbulent kinetic energy [m^2s^{-2}] for 3 ribs, *SR* = 0.5, Re = 16000, *H/w* = 11, *P* = 0.1

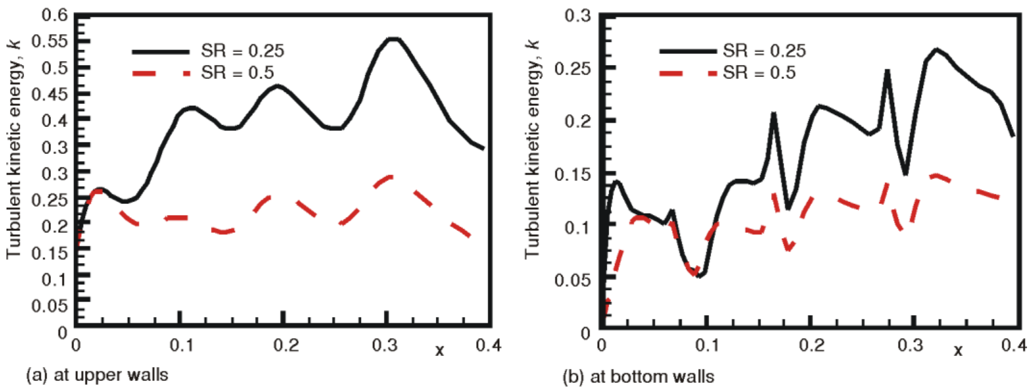

Figure 8. Effect of Re on variation of turbulent kinetic energy [m^2s^{-2}] for 3 ribs, *SR* = 0.5, Re = 16000, *H/w* = 11, *P* = 0.1

In fig. 9, the variation of local Nusselt number is seen. The local Nusselt number is increased with the increase of SR for 2 and 3 ribs at the region near the step. Also the Nusselt number is enhanced with the decrease of SR for the ribbed region as shown in (a). The presence of ribs will promote the convection heat transfer due to increase of the turbulence mixing. However the Nusselt number is decreased at the second rib. This will change when the number of ribs are increased to three as shown in (b). The turbulent kinetic energy is enhanced with increasing of Re as shown in fig. 10.

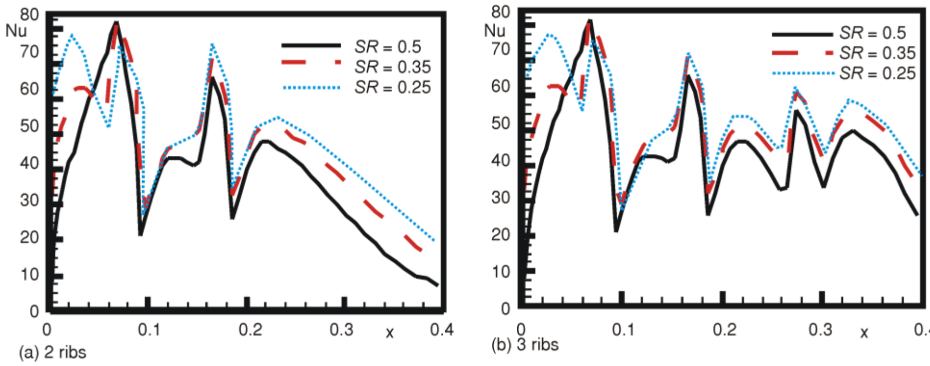

Figure 9. Effect of contraction ratio on variation of Nu for Re = 16000, *H/w* = 11, *P* = 0.1

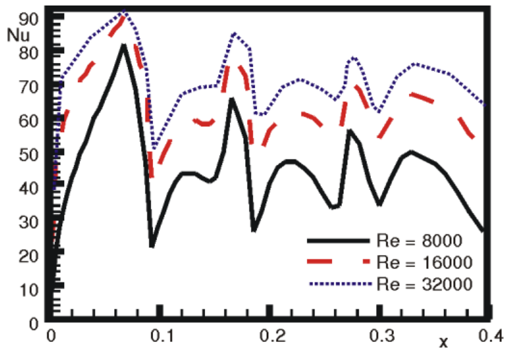

Figure 10. Effect of Re on variation of local Nu for 3 ribs, *SR* = 0.5, *H/w* = 11

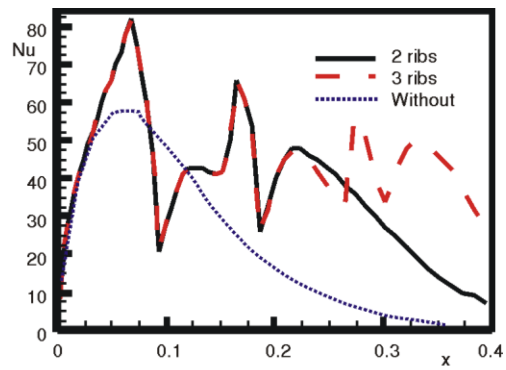

Figure 11. Comparison of variation of local Nu for the studied cases, *SR* = 0.5, Re = 16000, *H/w* = 11

The thermal performance of a backward-facing without ribs is compared with our problem as in fig. 11. The values of Nu are enhanced at the recirculation just after the edge of the step after that Nu is linearly decreased. While with ribs, the rate of heat transfer is significantly enhanced and the values of Nu are shifted and there is no difference between two and three ribs. However at the third rib, the value of Nu is increased.

The variation of Nu for different values of *SR* is found in fig. 12 for 2 ribs. The values of Nu are increased with the decrease

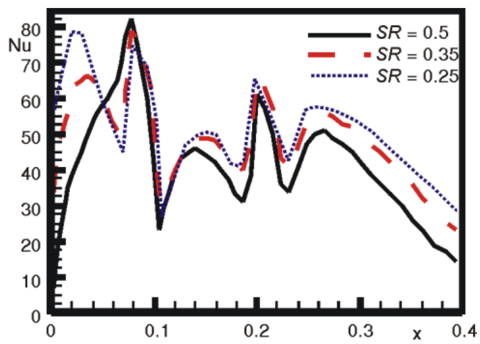

Figure 12. Effect of contraction ratio on variation of Nu for 2 ribs, *H/w* = 11, Re = 16000

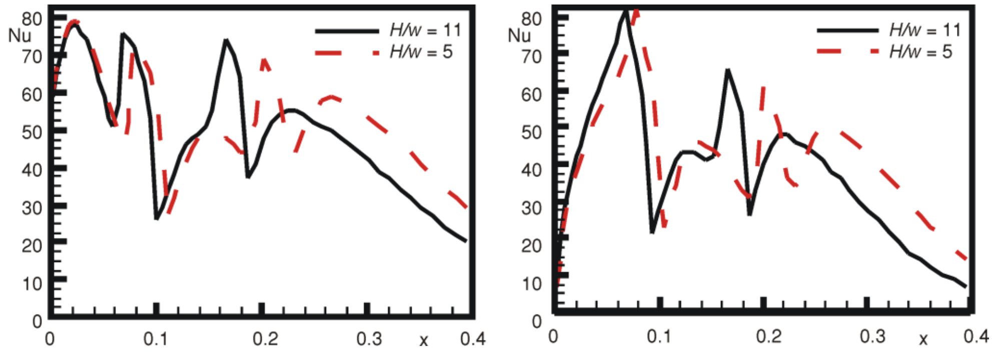

Figure 13. Effect of the rib width on Nu variation for Re 16000

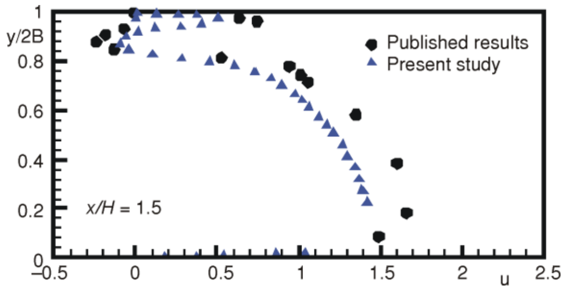

Figure 14. Comparison between the present simulation and published experimental data (published results of Lio *et al.* [10], *H/B* = 1, Re = 6000)

of SR for the region containing the ribs and *vice versa*. The cause arises to the increase of turbulence and that leads to incrase the rate of heat transfer. The effect of increasing of the rib width on heat transfer is shown in fig. 13 for different values of SR. It is evident that the rate of heat transfer is enhanced after the second rib and *vice versa* occurs at the step region.

The validation of the present code is examined through the comparison of the present results with available published experimental data as depicted in fig. 14. The comparison indicated an acceptable agreement.

Conclusions

The present study was performed for different values of Re, ribs turbulators, and step height. A finite volume based on the staggered method is used to simulate the backward--facing step flow with ribs turbulators. Thus, the following concluding remarks can be reported.

– Adding of the ribs turbulators to the backward-facing step flow is significantly enhanced the rate of heat transfer for the all studied Reynolds numbers.
– The strength and size of recirculation zones at the step and after the ribs is increased with the increase of Re. However this increase is larger after the first rib.
– The strength and size of recirculation zones are increased with the increase of *SR* ($0.25 \leq SR \leq 0.5$).
– The turbulent kinetic energy near the walls is decreased with the increase of *SR*.
– The numerical analysis shows that the heat transfer is increased with the increase of Re and *SR* and when using more ribs.
– The local Nusselt number decreases as the rib width increases.

Nomenclature

G	– generation term, [kgms^{-3}]
H	– height of the channel, [m]
k	– turbulent kinetic energy,[m^{-2}s^{-2}]
L	– length of the channel, [m]
Nu	– local Nusselt number, [–]
P	– pitch, [m]
p	– pressure, [Nm^{-2}]
Pr	– Prandtl number, [–]
Re	– Reynolds number, [–]
s	– step height, [m]
SR	– contraction ratio (= S/H), [–]
S_ϕ	– source term, [–]
T_c	– cold wall temperature, [°C]
T_h	– hot wall temperature, [°C]
u, v	– axial and normal velocity, [ms^{-2}]
x, y	– Cartesian co-ordinates, [m]

Greak letters

Γ_{eff}	– effective exchange coefficient,[kgms]
ε	– turbulence dissipation rate, [m^{-2}s^{-3}]
μ	– dynamic viscosity, [Nsm^{-2}]
μ_t	– turbulent viscosity, [Nsm^{-2}]
ρ	– air density, [Kgm^{-3}]
$\sigma_k, \sigma_\varepsilon$	– turbulent Schmidt numbers, [–]
θ	– dimensionless temperature [=$(T - T_c)/(T_h - T_c)$, [–]
ϕ	– constant property, [–]

References

[1] Lio, T., Hwang, J., Developing Heat Transfer and Friction in a Ribbed Rectangular Duct with Flow Separation at Inlet, *ASME J. Heat Transfer, 114* (1992), 3, pp. 546-573
[2] Wang, B., Zhang, H. Q., Wang, X. L., Large Eddy Simulation of Particle Response to Turbulence Along its Trajectory in a Backward-Facing Step Turbulent Flow, *Int. J. Heat and Mass Transfer, 49* (2006), 1-2, pp. 415-420
[3] Nie, J. H., Armaly, B. F., Three Dimensional Convective Flow Adjacent to a Backward Facing Step-Effects of Step Height, *Int. J. Heat Mass Transfer, 45* (2002), 12, pp. 2431-2438
[4] Thangam, S., Knight, D., Effect of Step Height on the Separated Flow Past a Backward Facing Step, *Phys. Fluids, 1* (1989), 3, pp. 604-606
[5] Chen, Y. T., *et al.*, Three Dimensional Convective Flow Adjacent to Inclined Backward Facing Step, *Int. J. Heat and Mass Transfer, 49* (2006), 25-26, pp. 4795-4803
[6] Feng, K. E., Liu, Y.-Z., Chen, H.-P., Simultaneous Flow Visualization and Wall Pressure Measurement of the Turbulent Separated and Reattachment Flow over a Backward Facing Step, *Journal of Hydrodynamics, 19* (2007), 2, pp. 108-187
[7] Han, J. C, Heat Transfer and Friction Characteristics in Rectangular Channels with Rib Turbulators, *ASME Journal of Heat Transfer, 110* (1988), 2, pp. 91-98
[8] Rau, G., *et al.* ,The Effect of Periodic Ribs on the Local Aerodynamics and Heat Transfer Performance of a Straight Cooling Channel, *ASME Journal of Turbo machinery, 120* (1988), 2, pp. 368-375
[9] Webb, R. L, Eckert, E. R. G., Goldsten, R. J., Heat Transfer and Friction in Tubes with Repeated Rib Roughness, *International Journal of Heat and Mass Transfer, 14* (1984), 4, pp. 601-617
[10] Liou, T. M., Hwang, G. G., Chen, S. H., Simulation and Measurements of Enhanced Turbulent Heat Transfer in Channels with Periodic Ribs on One Principal Wall", *International Journal of Heat Mass Transfer, 36* (1997), 2, pp. 507-507
[11] Han, J. C., Park, J. S., Developing Heat Transfer through Rectangular Channels with Rib Turbulators, *International Journal of Heat mass Transfer, 31* (1988), 1, pp. 183-194
[12] Tsai, W. B, Lin, W. W, Chieng, C. C., Computation of Enhanced Turbulent Heat Transfer in a Channel with Periodic Ribs, *Int. J. of Numerical Methods for Heat and Fluid Flow, 10* (2000), 1, pp. 47-66
[13] Lacovides, H., *et al*., Flow and Heat Transfer in a Rotating U-Bend with 45° Ribs, *Int. J. Heat and Fluid Flow, 22* (2001), 3, pp. 308-314
[14] Jones, W. P., Lunder, B. E., The Prediction of Laminarization with a Two Equation Model of Turbulence, *International Journal on Heat and Mass Transfer, 15* (1972), 2, pp. 301-314
[15] Versteege, H. K., Malalasekera, W., An Introduction of Computational Fluid Dynamics, Hemisphere Publishing Corporation, Washington, D. C., USA, 1995

Paper submitted: September 26, 2009
Paper revised: May 4, 2010
Paper accepted: February 25, 2010